Vacuum-Evaporated Cavitand Sensors: Dissecting Specific from Nonspecific Interactions in Ethanol Detection

Michele Tonezzer,*[,†,‡] Monica Melegari,[§] Gianluigi Maggioni,[‡] Riccardo Milan,[†] Gianantonio Della Mea,[†,‡] and Enrico Dalcanale*[,§]

Università di Trento, Dipartimento di Ingegneria dei Materiali e Tecnologie Industriali, Via Mesiano 77, 38050 Povo (TN), Italy, Istituto Nazionale di Fisica Nucleare, Laboratori Nazionali di Legnaro, Viale dell'Università 2, 35020 Legnaro, Padova, Italy, and Dipartimento di Chimica Organica ed Industriale and INSTM, UdR Parma, Viale Usberti 17/A, 43100 Parma, Italy

Received June 30, 2008. Revised Manuscript Received September 4, 2008

High vacuum evaporation (VE) is used for the first time to grow thin films of novel tetraphosphonate, **Tiiii[H, CH_3, Ph]**, and tetrathiophosphonate, **TSiiii[H, CH_3, Ph]**, cavitands for gas sensing applications. The sublimation rate of the compounds was monitored during the depositions and related to the final physical properties of the samples. The properties of deposited films were investigated by various techniques. FT-IR and ESI-MS indicate that the samples consist of pristine cavitand molecules and demonstrate the high purity of the VE films. AFM images show the **Tiiii** and **TSiiii** films to possess similar thickness and globular morphology. These physical analyses indicate the uniformity and homogeneity of the final samples as well as the high reproducibility of the VE technique. The sensing capabilities of the samples were investigated by exposing **Tiiii**- and **TSiiii**-coated QCMs to ethyl alcohol in very low concentrations. The sensitivity, the speed, and the detection limit of the samples were determined, indicating highly competitive sensing capabilities. Elovich kinetics and Langmuir−Henry isotherms were used to analyze the sorption process occurring onto the different samples and showed that, whereas **TSiiii** samples consist mainly of unspecific adsorption sites, **Tiiii** films show specific active sites where analyte molecules can be trapped and detected.

1. Introduction

Chemical sensing requires an integrated approach, where both the molecular and the materials properties of the sensing layer must be finely tuned to achieve the desired properties. In the specific case of supramolecular sensing,[1] the main focus to date has been on the molecular design of the receptor as a function of the analytes to be detected. The material side has been largely neglected, despite its great influence on the ultimate performances of the sensors. In this respect, supramolecular sensing of gases and vapors represents a particular challenge, as the desired recognition events need to operate at the gas−solid interface.[2] Because analyte recognition is mediated by the layer properties of the coated receptors, precise control and accurate characterization of these properties (e.g., thickness, permeability, and morphology) are critical for developing advanced sensing materials.

Cavitands,[3] together with cyclodextrins[4] and calixarenes,[5] are the most studied receptors for gas/vapor sensing because of their outstanding host−guest properties, which are tunable for the recognizing of different classes of analytes. For exploitation as sensing materials, these compounds are usually deposited as thin solid films. Standard production methods for obtaining thin solid films from cavitand molecules utilize wet deposition; in particular, spray-[6] and spin-coating[7] methods are commonly employed. Nevertheless, despite promising results for cavitands as chemical receptors, these deposition methods suffer from several drawbacks such as inhomogeneous surface morphology (for spray coating)[2] and uncontrollable thickness. Moreover, insoluble compounds cannot be deposited by such solution techniques. To date, the most common method of depositing insoluble compounds by solution techniques consists of decorating them with peripheral alkyl chains to improve their solubility. This molecular derivatization introduces dispersion interactions that dilute or even completely obscure the specific analyte response, significantly decreasing sensor selectivity.[8]

As alternatives, Langmuir−Blodgett and Langmuir−Schafer deposition methods provide ordered and reproducible monolayers, which are very effective when the sensitivity of the

* To whom correspondence should be addressed. E-mail: tonezzer@lnl.infn.it (M.T.); enrico.dalcanale@unipr.it (E.D.).
† Universitá di Trento.
‡ Laboratori Nazionali di Legnaro.
§ UdR Parma.

(1) Lavigne, L. L.; Anslyn, E. V. *Angew. Chem., Int. Ed.* **2001**, *40*, 3118.
(2) Pirondini, L.; Dalcanale, E. *Chem. Soc. Rev.* **2007**, *36*, 695.
(3) Cram, D. J.; Cram, J. M. *Container Molecules and Their Guests*; Stoddart, J. F., Ed.; The Royal Society of Chemistry: Cambridge, U.K., 1994.
(4) (a) Hierlemann, A.; Ricco, A. J.; Bodenhoefer, K.; Göpel, W. *Anal. Chem.* **1999**, *71*, 3022. (b) Kieser, B.; Fietzek, C.; Schmidt, R.; Belge, G.; Weimar, U.; Schurig, V.; Gauglitz, G. *Anal. Chem.* **2002**, *74*, 3005.
(5) Gutsche, C. D.; *Calixarenes*; Stoddart, J. F., Ed.; The Royal Society of Chemistry: Cambridge, U.K., 1989.
(6) Hartmann, J.; Hauptmann, P.; Levi, S.; Dalcanale, E. *Sens. Actuators, B* **1996**, *35−36*, 154.
(7) Feresenbet, E. B.; Dalcanale, E.; Dulcey, C.; Shenoy, D. K. *Sens. Actuators, B* **2004**, *97*, 211.
(8) Di Natale, C.; Paolesse, R.; Macagnano, A.; Nardis, S.; Martinelli, E.; Dalcanale, E.; Costa, M.; D'Amico, A. *J. Mater. Chem.* **2004**, *14*, 1281.

10.1021/cm801778f CCC: $40.75
Published on Web 10/04/2008

Chart 1. Structures (above) and 3D CPK Models (below) of Tetraphosphonate Tiiii[H,CH_3,Ph] and Tetraphosphoante TSiiii[H,CH_3,Ph] Cavitands

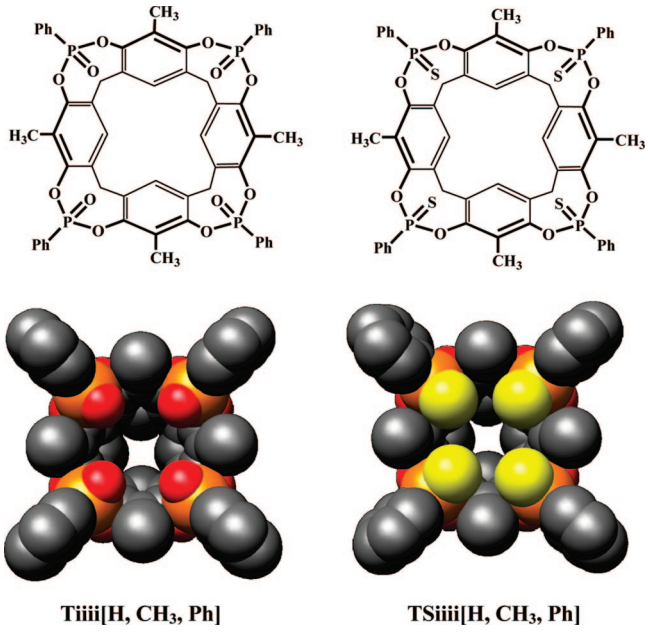

transducer is adequate.[9] However, when a bulk response is required by the sensing layer, such as in quartz crystal microbalances (QCM), deposition of highly permeable, amorphous coatings is necessary.

The compounds employed in this work are the tetraphosphonate (**Tiiii**) and tetrathiophosphonate (**TSiiii**) cavitands depicted in Chart 1.They present an open, conformationally rigid cavity, delimited by four inward oriented P═O/P═S bridging groups at the upper rim.[10] The structure of these cavitands is born out by previous studies on the sensing properties of tetraphosphonate cavitands toward short chain alcohols.[11] Substitution of the four P═O groups with the P═S moieties completely prevents complexation by eliminating H-bonding interactions between the cavitand and the analyte. The structural similarity of the two cavitands allows for a valid comparison of the influence of molecular recognition on sensing performance. Two structural variations of previously described cavitands[11] were implemented in this study: (i) the four alkyl chains at the lower rim were removed, to minimize nonspecific interactions; and (ii) four methyl groups were introduced in the apical positions to deepen the cavity and increase the strength of CH−π interactions. The first modification necessitates a different film deposition method, because both cavitands are too insoluble to be deposited by either spray- or spin-coating.

High-vacuum evaporation (VE) overcomes solubility problems, allowing for the direct formation of films from solid materials. The lack of residual solvent during the deposition process assures the formation of high purity films: this represents a basic requirement in the gas sensing field, because of the unpredictable effects of the retained solvent on the final response of the sensor, including occupation of adsorption sites and interference in analyte/material interactions.[12] In this regard, recent studies have demonstrated that vacuum-evaporated thin films exhibit higher gas sensing capabilities toward alcohol vapors than chemically deposited films.[13,14]

Moreover, VE technique is characterized by good reproducibility, high uniformity, and homogeneity and provides accurate control over both the growth rate and the final thickness of the samples.

In this paper, we report the employment of the VE technique for producing **Tiiii**- and **TSiiii**-sensing coatings. Because this is the first time that cavitand solid films have been deposited by vacuum sublimation, an in-depth characterization of the deposition process and of the properties of the samples was conducted.

We studied the deposition rate of the different cavitand molecules as a function of crucible temperature by in situ QCM. The potential degradation of the sublimated molecules, as well as the purity of the films, were monitored by Fourier transform infrared (FT-IR) and electrospray ionization mass spectrometry (ESI-MS). Atomic force microscopy (AFM) analyses were performed to investigate the morphological features and the thickness of the samples.

The sensing capabilities (i.e., sensitivity, response speeds, and recovery degree) of the **Tiiii**- and **TSiiii**-coated QCMs toward ethyl alcohol were thoroughly studied by exposing them to several fluxes in a low concentration range (5−200 ppm), and their limits of detection were evaluated. Moreover, their responses were analyzed through Elovich kinetics and Langmuir−Henry isotherms highlighting notable differences between the sorption processes of the two cavitand coatings.

2. Experimental section

2.1. Chemicals and Synthesis. All commercial reagents were ACS reagent grade and were used as received. The resorcinarene scaffold was prepared according to a published procedure.[15] Long chain footed cavitand **Tiiii[$C_{11}H_{23}$, H, Ph]**, used for sensing comparison, was likewise prepared as described previously.[11]

Cavitand ***T_{iiii}[H, CH_3, Ph].*** Dichlorophenylphosphine (1.02 mL, 7.49 mmol) and pyridine (1.22 mL, 1.51 mmol) were added, under nitrogen, to a solution of resorcinarene (1.0 g, 1.84 mmol) in 40 mL of anhydrous DMA. After 1 h, a mixture of H_2O_2/$CHCl_3$ was added dropwise and the reaction was vigorously stirred for 1 h. The $CHCl_3$ was removed under vacuum and the resulting precipitate was filtered and washed with water (3 × 30 mL). The solid was treated with 200 mL of water, sonicated, filtered, and dried under a vacuum to yield the desired compound as white solid (1.79 g,

(9) (a) Shenoy, D. K.; Feresenbet, E. B.; Pinalli, R.; Dalcanale, E. *Langmuir* **2003**, *19*, 10454. (b) Feresenbet, E. B.; Busi, M.; Ugozzoli, F.; Dalcanale, E.; Shenoy, D. K. *Sens. Lett.* **2004**, *2*, 186. (c) Daly, S. M.; Grassi, M.; Shenoy, D. K.; Dalcanale, E. *J. Mater. Chem.* **2007**, *17*, 1809.

(10) For the nomenclature adopted for phosphonate cavitands see: Pinalli, R.; Suman, M.; Dalcanale, E. *Eur. J. Org. Chem.* **2004**, 451.

(11) Melegari, M.; Suman, M.; Pirondini, L.; Moiani, D.; Massera, C.; Ugozzoli, F.; Kalenius, E.; Vainiotalo, P.; Mulatier, J.-C.; Dutasta, J.-P.; Dalcanale, E. *Chem.—Eur. J.* **2008**, *14*, 5772.

(12) Tonezzer, M. Ph.D. Thesis, University of Trento, Trento, Italy, 2007.

(13) Tonezzer, M.; Maggioni, G.; Quaranta, A.; Carturan, S.; Della Mea, G. *Sens. Actuators, B* **2007**, *122*, 613.

(14) Tonezzer, M.; Quaranta, A.; Maggioni, G.; Carturan, S.; Della Mea, G. *Sens. Actuators, B* **2007**, *122*, 620.

(15) Konishi, H.; Iwasaki, Y.; Okano, T.; Kiji, J. *Chem. Lett.* **1989**, 1815.

93%). ^{1}H NMR ($CDCl_3$/MeOD, 300 MHz): δ 8.16−8.09 (m, 8H, POArH_o), 7.63−7.52 (m, 12H, POArH_m + POArH_p), 7.09 (s, 4H, ArH_{down}), 4.52 (d, 4H, ^{2}J=13 Hz, $Ar_2CH_{eq.}$), 3.51 (d, 4H, ^{2}J=13 Hz, $Ar_2CH_{ax.}$), 2.28 (s, 12H, ArCH_3). ^{31}P NMR ($CDCl_3$, 162 MHz) δ = 4.82 (s, 4P, *P*OPh). ESI-MS: *m/z* 1055.4 $[M + Na]^+$.

Cavitand ***TS$_{iiii}$[H, CH$_3$, Ph].*** Dichlorophenylphosphine (1.02 mL, 7.49 mmol) and pyridine (1.22 mL, 1.51 mmol) were added, under nitrogen, to a solution of resorcinarene (1.0 g, 1.84 mmol) in 40 mL of anhydrous DMA. After 1 h, S_8 (0.98 g, 1.28 mmol) was added and the reaction was stirred for 1 h at 50 °C. The resulting precipitate was filtered and washed with water (3 × 30 mL). The solid was treated with 200 mL of water, sonicated, filtered, and dried under a vacuum to yield the desired compound as white solid (1.49 g, 89%). ^{1}H NMR ($CDCl_3$, 300 MHz): δ 8.22−8.16 (m, 8H, PSArH_o), 7.59−7.52 (m, 12H, PSArH_m + PSArH_p), 6.89 (s, 4H, ArH_{down}), 4.45 (d, 4H, ^{2}J=13 Hz, $Ar_2CH_{eq.}$), 3.54 (d, 4H, ^{2}J=13 Hz, $Ar_2CH_{ax.}$), 2.09 (s, 12H, ArCH_3). ^{31}P NMR ($CDCl_3$, 162 MHz): δ = 74.55 (s, 4P, *P*SPh). ESI-MS: *m/z* 1097.3 $[M + H]^+$, 1119.3 $[M + Na]^+$, 1135.3 $[M + K]^+$.

2.2. Evaporation Apparatus. The experimental equipment used for the evaporation of the cavitand molecules comprises a stainless steel vacuum chamber, evacuated by a turbo molecular pump to a base pressure of 1×10^{-4} Pa. The chamber is equipped with a copper crucible wrapped with a heating wire (maximum temperature 500 °C), which was filled with the cavitand. The deposition equipment is supplied with a movable shutter: it was held open once the deposition temperature of the crucible was achieved, while during the heating and the cooling phases, it was held between the crucible and the sample holder. In this way, the uncontrolled deposition of organic molecules onto the substrates was prevented.

The deposition rate and film thickness were measured by a quartz crystal microbalance thickness sensor (Sycon) positioned in the center of the sample holder.

The films were deposited on two different substrates depending on the analytical method: P-doped (1 0 0) silicon wafers lapped on both faces (Bayville Chemical Co.) for FT-IR, AFM, and ESI-MS analyses, and QCM for sensing measurements. The substrates were placed on a fixed sample holder positioned 10 cm above the crucible and were maintained at room temperature during the deposition process.

2.3. Film Characterization. FT-IR spectra of the samples were recorded in the 4000−400 cm^{-1} range using a Jasco FTIR 660 Plus spectrometer with a resolution of 16 cm^{-1}. During the measurements, the sample cell and the interferometer were evacuated in order to remove from the spectra the absorption peaks of water and atmospheric gases.

ESI-MS characterization experiments were performed on a Waters ACQUILITY SQD Detector equipped with a ESCi multi mode ionization (APCI/ESI).

The surface morphology of the organic samples was investigated in air by a no-contact-mode atomic force microscope (AFM) model C-21 (Danish Micro Engineering), mounting a DualScope Probe Scanner 95−50. For each sample, several images were acquired from different positions and acquired with different scan sizes ranging from 1×1 μm^2 to 50×50 μm^2 in order to verify the uniformity and homogeneity of the samples.

AFM measurements were also utilized to investigate the thickness of the samples by scratching a small area of the samples with a doctor blade and then acquiring an image of the borderline between the exposed substrate and the pristine film.

All the images were acquired in AC mode at a very slow speed, typically under 1 μm/s. The observations were performed with a Si_3N_4 pyramidal tip with a curvature radius lower than 50 nm. The images were analyzed and processed using the standard software supplied with the control electronics.

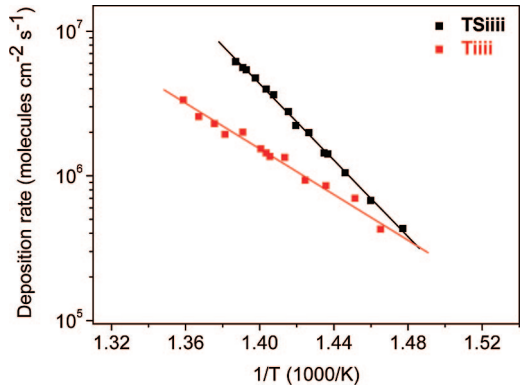

Figure 1. Deposition rates of **TSiiii** and **Tiiii** vs temperature.

2.4. Sensing Measurements. Sensing measurements were performed using AT-cut quartzes with a fundamental frequency of 10 MHz and a crystal diameter of 8 mm. Thin cavitands films were vacuum-evaporated on both sides of the quartz transducers.

QCM sensors are mass transducers where the frequency of oscillation, for small increases of mass, is governed linearly by the Sauerbrey equation[16]

$$\Delta f = k_k \Delta m \quad (1)$$

where the Δf is the frequency variation of a Δm increase in mass.

The quartz constant is experimentally estimated to be $k_q = -0.46$ Hz ng^{-1}. This value provides a nominal mass resolution of 1.6 ng Hz^{1-},[17] considering a minimum reliable frequency measurement of 1 Hz.

To control the amount of the deposited cavitand films, we monitored QCM frequency online during the deposition process by a high stability frequency counter. A total frequency variation of $\Delta f = -20 \pm 0.5$ kHz was obtained for all samples produced.

The measurement system (Gaslab 20.1; IFAK, Magdeburg) is equipped with a flow chamber, containing four coated quartz crystals, a reference quartz crystal and a thermocouple. The chamber was thermostatted at 20 ± 0.1 °C. The QCM chamber is connected with two mass-flow controllers (Brooks 5850S): one allows control over the flow rate of ethanol mixture from 2 to 50 mL/min and the other controls the flow rate of pure nitrogen from 150 to 200 mL/min. The initial stream of N_2 (200 ± 2 mL/min) was replaced by a N_2 + EtOH mixture (200 ± 2 mL/min); the precise N_2/EtOH ratio is determined by the desired final alcohol concentration, given that the total flow rate of the stream must be 200 ± 2 mL/min. After attaining a flat characteristic plateau (equilibrium of partition coefficient), the chamber was flushed with pure N_2 to restore the starting conditions. Throughout the whole process, the coated quartz crystal frequency was measured as a function of the time every 1 s. All measurements were repeated at least four times, with variations in response less than 3%. The ethanol vapor was supplied by SAPIO Srl in gas cylinders with a certified concentration of 504 ppm. The graduated cylinders were prepared following the standard gravimetric procedure of the normative ISO 6142.

3. Results and Discussion

3.1. Film Deposition. Figure 1 shows the plots of the deposition rates of the **Tiiii** and **TSiiii** compounds vs the

(16) Ballatine, D. S.; White, R. M.; Martin, S. J.; Ricco, A. J.; Zellers, E. T.; Frye, G. C.; Wihltjen, H. *Acoustic Wave Sensors*; Academic Press: San Diego, 1997.
(17) Öztürk, Z. Z.; Zhou, R.; Weimar, U.; Ahsen, V.; Bekaroglu, O.; Göpel, W. *Sens. Actuators, B* **1995**, *26−27*, 208.

reciprocal crucible temperature. The deposition rates were evaluated as the number of molecules deposited per unit of surface area and time (molecules cm^{-2} s^{-1}) by normalizing the readings of the thickness sensor to the molecular weight of each compound. Each curve can be fit by the following function[18]

$$\log D = A - \frac{B}{T} \quad (2)$$

where D is the deposition rate, T is the absolute temperature, and A and B are constants determined from the fits. For **Tiiii**, $A = 25.5$ and $B = 8378$ K; and for **TSiiii**, $A = 32.6$ and $B = 12\,817$ K.

Vacuum evaporation assures a strictly controlled and reproducible deposition process. In fact, the deposition rate can be accurately adjusted through the crucible temperature and sample growth is easily verifiable through in situ QCM analysis, both in terms of deposition rates and the final deposited mass.

The same production parameters were adopted for the deposition of **Tiiii** and **TSiiii** films: the distance between the cavitand-containing crucible and the substrates was fixed at 10 cm and the base pressure into the chamber was kept at 2×10^{-4} Pa. The crucible temperature was maintained at 440 °C over the entire deposition process. As reported in Figure 1, at this temperature the deposition rate of **TSiiii** ($D = 1.54 \times 10^{14}$ molecules cm^{-2} s^{-1}) is approximately three times higher than that of **Tiiii** ($D = 5.7 \times 10^{13}$ molecules cm^{-2} s^{-1}). These different deposition rates can be explained by taking into account the polarity of the two cavitands. In fact, **TSiiii**, being less polar than **Tiiii**, is characterized by lower intermolecular interactions, and requires less thermal energy to sublimate.

3.2. Chemical Characterization of the Cavitand Films. FT-IR and ESI-MS analyses were conducted to investigate the purity of the sublimated films and to exclude the presence of impurities derived from cavitand decomposition.

The infrared spectra of **Tiiii** and **TSiiii** films are shown in Figure 2: the spectra of the respective powders are reported as references. The IR bands, as well as their vibrational assignments,[19,20] are summarized in Table S1 in the Supporting Information. **Tiiii** and **TSiiii** samples are characterized by similar infrared spectra due to the close resemblance of their molecular structures: nevertheless, differences in certain positions is noteworthy. In particular, **Tiiii** shows a diagnostic peak at 1272 cm^{-1} assigned to the (P═O) stretching vibration, while the corresponding **TSiiii** (P═S) stretching vibration is shifted to 1312 cm^{-1}. Both **Tiiii** and **TSiiii** samples show all the characteristic peaks of the respective powders, indicating the absence of damaged molecules in both the VE samples, within the detection limits of the techniques employed. Moreover, the lack of any additional peaks in the FT-IR spectra excludes the presence of extraneous compounds, demonstrating the high purity of the samples. As additional evidence, optical inspection and FT-IR analysis of the residual cavitands left into the crucible showed no evidence of decomposition.

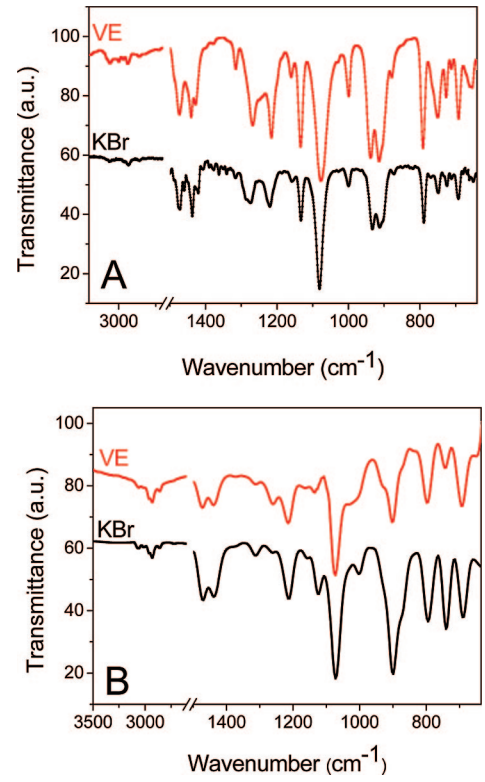

Figure 2. FT-IR spectra of vacuum evaporated films (VE) of (A) **Tiiii** and (B) **TSiiii** cavitands. The spectra of the corresponding starting powders pressed in KBr pellet (KBr) are also reported as reference.

The integrity of the cavitand molecules which compose the sublimated films, as well as the purity of the samples, were confirmed by ESI-MS analyses. In fact, the spectra of the VE films and that of starting powders show no differences (see Figures S1and S2 in the Supporting Information). These results are in agreement with previous works in which the high purity of physically deposited organic films has been proved[13,14,21] and demonstrate the viability of the VE technique for the deposition of thermally stable molecular receptors.

3.3. Physical Characterization of the Cavitand Layers. AFM measurements of vacuum-evaporated **Tiiii** and **TSiiii** coatings were performed in order to investigate the topography and the surface roughness of the vacuum-evaporated samples. AFM images of **Tiiii** and **TSiiii** coatings are reported in Figure 3.

Both the **Tiiii** and **TSiiii** films show surface morphologies consisting of numerous globe-like molecular aggregations, differing in terms of the globe sizes. The AFM images show that the **Tiiii** surfaces present smaller globular aggregations than the **TSiiii** surfaces, even though few larger islands also appear. As a result of their different morphologies, **TSiiii** films show an average square roughness slightly larger than

(18) Pethe, R. G.; Carlin, C. M.; Patterson, H. H.; Unertl, W. N. J. *Mater. Res.* **1993**, *8*, 3218.
(19) Zhang, Y. H.; Ruan, W. J.; Li, Z. Y.; Zheng, Y. W. *Chem. Phys.* **2005**, *315*, 201.
(20) Furer, V. L.; Vandyukov, A. E.; Majoral, J. P.; Caminade, A. M.; Kovalenko, V. I. *Spectrochim. Acta, A* **2004**, *60*, 1649.
(21) (a) Maggioni, G.; Quaranta, A.; Carturan, S.; Patelli, A.; Tonezzer, M.; Ceccato, R.; Della Mea, G. *Chem. Mater.* **2005**, *17*, 1895. (b) Maggioni, G.; Quaranta, A.; Carturan, S.; Patelli, A.; Tonezzer, M.; Ceccato, R.; Della Mea, G. *Surf. Coat. Technol.* **2005**, *200*, 476.

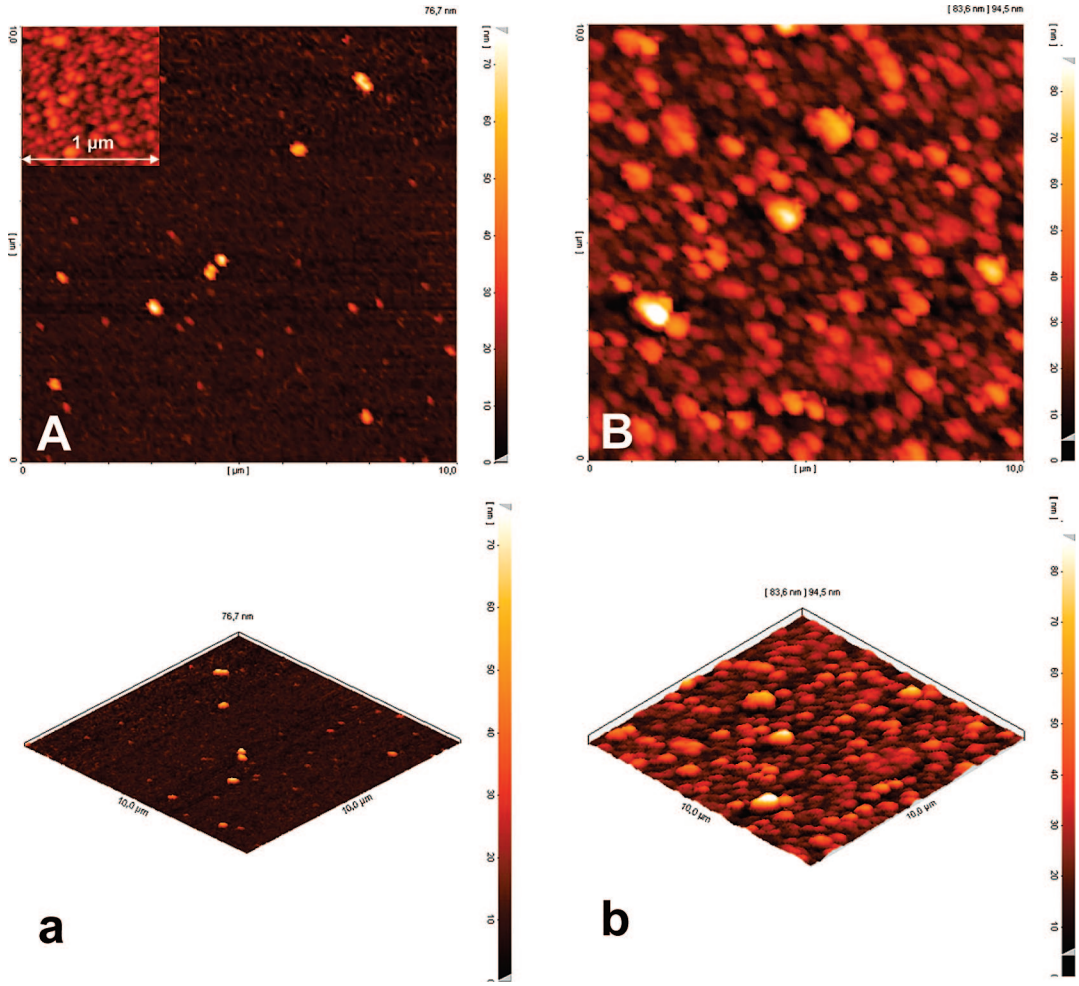

Figure 3. AFM images of vacuum evaporated films. Plane view and 3D view of (A,a) **Tiiii** and (B,b) **TSiiii** surfaces. In the inset of (A), the plane view AFM image of **Tiiii** at higher magnification (1 × 1 μm) is reported.

Table 1. Average Roughness, Lateral Dimensions and Heights of the Surface Islands, and Thickness of the TSiiii and Tiiii Vacuum-Evaporated Films

	Tiiii	**TSiiii**
roughness (nm)	4.4	10.7
island lateral dimension (nm)	60	420
island height (nm)	5	15
thickness (nm)	355	340

Tiiii films. The sizes of the surface globes, as well as the surface roughness of the samples, were evaluated by AFM and reported in Table 1.

The different globular structures of the **Tiiii** and **TSiiii** coatings suggest different modes of growth in the production of the two samples. In particular, the deposition rate is suspected to influence the final structure of the films: As the rate of film deposition increases, less time is available for surface molecules to reach their thermodynamic equilibrium positions before being trapped by the arrival of subsequent molecules. Thus, the higher deposition rate for **TSiiii** samples implies a rougher surface morphology than **Tiiii** samples, for which the deposition rate is lower.

The thickness of the **Tiiii** and **TSiiii** films was also investigated by AFM. These measurements reveal that sublimated **Tiiii** and **TSiiii** samples are characterized by very similar thicknesses.

The roughness and the thickness of the samples are reported in Table 1. It is notable that these properties were found to be the same over the entire sample surface and for several analytic magnifications, demonstrating the high uniformity and homogeneity of the VE coatings. Moreover, processes conducted with the same deposition parameters produced samples with the same physical properties, demonstrating the high reproducibility of the VE technique.

3.4. Sensing and Sorption Measurements. Sensing measurements were performed by exposing cavitand-coated QCMs to different concentrations (ranging from 5 to 200 ppm) of ethyl alcohol (EtOH) and monitoring the shift of the QCM fundamental resonance frequency induced by the mass changes as a function of time. EtOH was chosen for this testing because its mode of interaction with **Tiiii** is well-understood[11] and because selective EtOH sensors are of technological relevance for the food industry. By injecting EtOH vapors into the gas flow, the responses of the **Tiiii** and **TSiiii** coated sensors are reproducible, reversible, and rapid. The recovery capabilities of the samples are particularly significant considering that the measurements were conducted at 20 °C. In fact, many authors reported that it is necessary to heat organic samples to obtain complete recovery in reasonable times;[22] nevertheless, extended heat-

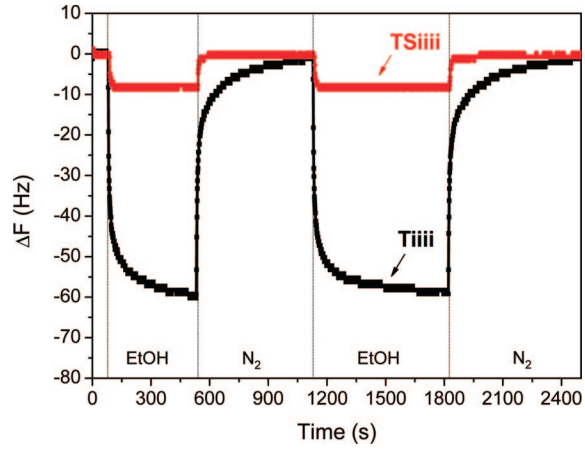

Figure 4. Change of the resonance frequency of **Tiiii** and **TSiiii** vacuum-evaporated samples as a function of time during exposure to 25 ppm EtOH. Both the response and recovery phases are performed at 20 °C.

ing procedures, causing thermal cycles in the samples, can degrade the organic films.

Figure 4 shows the time responses of **Tiiii** and **TSiiii** sensors exposed to 25 ppm of EtOH. It is evident that both samples exhibit a fast decrease of the resonance frequency within seconds, followed by a slower decrease until saturation values are reached. As the EtOH vapor stream was switched off, a dry nitrogen flux was activated, and after a few hundred seconds, the original resonance frequencies were restored. The most significant result is the high difference in response intensity between the samples: **Tiiii**-coated QCM shows a resonance frequency decrease ($\Delta F = -60$ Hz) eight times higher than that of **TSiiii** ($\Delta F = -7.5$ Hz). Previous studies have indicated that the following key factors affect the sensing performances of phosphorus-bridged cavitands toward alcohols: (i) the preorganized cavity which provides a free volume available for the analyte, pivotal for effective H-bonding;[23] (ii) the presence of synergistic CH$-\pi$ interactions with the π-basic cavity and the energetically equivalent H-bonding options between the P═O groups at the upper rim and the analyte (specific interactions).[24] The resulting mode of interaction between ethanol and the cavity shows how the ethanol chain fits into the cavity with its methyl residue (CH$-\pi$ interactions), while the OH moiety undergoes H-bonding interactions with the P═O groups. The effective contribution of the H-bonds is absent in the **TSiiii** cavitand, because the P═S is much less polarized than the P═O one and, consequently, it is ineffective as H-bond acceptor.[25] Therefore the observed **TSiiii** responses are due to nonspecific dispersion interactions between the organic layer and EtOH and the large difference in the sensor responses can be attributed to the specific binding of EtOH by the **Tiiii** cavitand.

Table 2. Response and Recovery Times of Tiiii and TSiiii Films upon Exposure to 25 ppm EtOH; Both the Response and Recovery Phases Have Been Performed at 20 °C

	response time (s)		recovery time (s)	
sample	t_{50}	t_{90}	t_{50}	t_{10}
Tiiii	4	78	5	152
TSiiii	5	12	5	15

To quantify the response speed of the samples, we measured the parameters t_{50} and t_{90}, defined as the times required for the signal intensity to reach 50 and 90% of its final saturated value. Similarly, the recovery speed was estimated with the parameters t_{50} and t_{10}, defined as the times required for the signal intensity to reach 50 and 10% of its saturated value during ethanol desorption. Table 2 reports the parameters observed for both samples. The response and recovery phases of both the samples are particularly fast compared to previous reports of organic gas-sensing materials at room temperature.[26] The **Tiiii** sensor shows t_{90} and t_{10} times that are slightly slower than the **TSiiii** ones, suggesting that different sorption processes are operative in the two different cavitand coatings.

To investigate the interaction between EtOH and the sublimated films, we analyzed the recovery phase of the samples by Elovich kinetics.[27] According to this model, the surface uncovering Θ during the recovery phase is governed as a function of time by the following formula

$$\Theta(t) = \frac{1}{\beta}\ln(t) + K \qquad (3)$$

where β and K are constants.

This model is based on the assumption that the desorption probability of an analyte molecule during surface purging decreases exponentially as a function of the number of analyte molecules already desorbed. Thus, by assuming that the resonant frequency (ΔF) is related only to the interaction between EtOH and cavitand coatings, the value of Θ should be proportional to ΔF. Hence, by plotting ΔF as a function of $\ln(t)$, a linear relationship should be obtained.

Figure 5 reports the plots of ΔF vs $\ln(t)$ for the recovery phases of the **Tiiii** and **TSiiii** layers, exposed to 5 and 100 ppm EtOH respectively. As can be observed, the trends of **Tiiii**- and **TSiiii**-coated QCMs are characterized by different behaviors. The **Tiiii** behavior is approximately linear over the first 10 s, deviating from linearity at higher times. This indicates a change in activation energy dependent on surface coverage, supporting a two-step interaction process:[28] (i) a weak interaction between analyte molecules and nonspecific sites and (ii) a stronger specific interaction due to cavity inclusion. In particular, the linear region represents the fast process during which EtOH molecules are removed from the nonspecific sites of the **Tiiii** coating, while the nonlinear region represents slow EtOH release from the specific sites of the layer. By contrast, the **TSiiii**-coated QCM shows a

(22) (a) Pedrosa, J. M.; Dooling, C. M.; Richardson, T. H.; Hyde, R. K.; Hunter, C. A.; Martin, M. T.; Camacho, L. *J. Mater. Chem.* **2002**, *12*, 2659. (b) Richardson, T. H.; Dooling, C. M.; Worsfold, O.; Jones, L. T.; Kato, K.; Shinbo, K.; Kaneko, F.; Treggoning, R.; Vysotsky, M. O.; Hunter, C. A. *Thin Solid Films* **2001**, *393*, 259.
(23) Paolesse, R.; Di Natale, C.; Nardis, S.; Magagnano, A.; D'Amico, A.; Pinalli, R.; Dalcanale, E. *Chem.—Eur. J.* **2003**, *9*, 5388.
(24) Pinalli, R.; Nachtigall, F. F.; Ugozzoli, F.; Dalcanale, E. *Angew. Chem., Int. Ed.* **1999**, *38*, 2377.
(25) Van Damme, D. R.; Zeegers-Huyskens, T. *J. Phys. Chem.* **1980**, *84*, 282.
(26) Dooling, C. M.; Worsfold, O.; Richardson, T. H.; Tregonning, R.; Vysotsky, M. O.; Hunter, C. A.; Kato, K.; Shinbo, K.; Kaneko, F. *J. Mater. Chem.* **2001**, *11*, 392.
(27) Elovich, S. Yu.; Zhabrova Zhur, G. M. *Fiz. Khim.* **1939**, *13*, 1761.
(28) Arnold, D. P.; Manno, D.; Micocci, G.; Serra, A.; Tepore, A.; Valli, L. *Langmuir* **1997**, *13*, 5951.

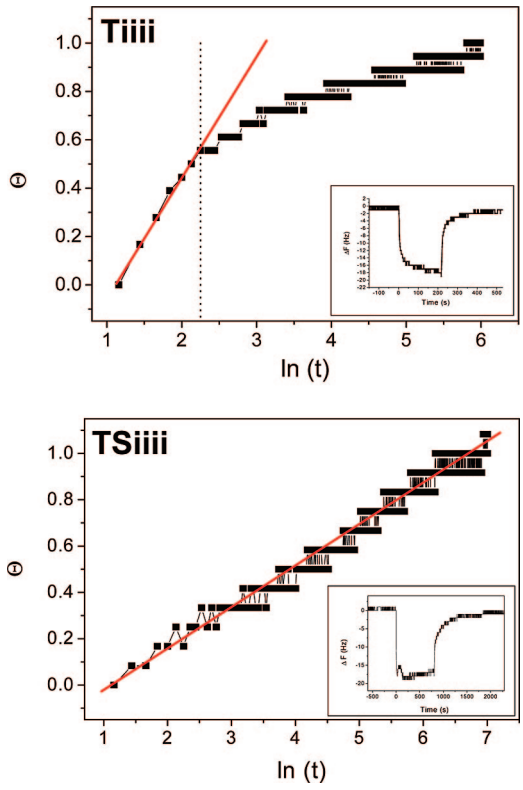

Figure 5. Elovich recovery kinetics for vacuum-evaporated **Tiiii** and **TSiiii** films after exposing to 5 and 100 ppm EtOH, respectively.

completely linear behavior, indicating an interaction process dominated totally by nonspecific dispersion interactions.

This result is in good agreement with the sensing results explained above. To validate this finding, we performed a thorough evaluation of the different interaction processes occurring in the samples by analyzing the responses through a combination of Langmuir- and Henry-type sorption isotherms. Different isotherm models can be used to analyze the sorption processes of analyte molecules onto a solid surface:[29] The Langmuir adsorption isotherm was found to be diagnostic of specific adsorption processes, such as molecular inclusion.

The effect of analyte concentration on the frequency change of the sensors was investigated with exposure-recovery cycles obtained over an EtOH range of 5−200 ppm. During all the exposures, the temperature was held at 20 ± 0.1 °C. The Langmuir curves of the **Tiiii** and **TSiiii** vacuum sublimated samples are plotted in Figure 6. Both cavitand-coated QCMs show higher responses at increased analyte concentrations. The trend, however, is completely different in the two cases, both in terms of the intensity and the profile. The much more pronounced responses of the **Tiiii** sensor layer are the result of complexation events occurring at the gas−solid interface.

By comparing the shapes of the two isotherms, interesting considerations on the different sorption processes can be conducted. The **Tiiii** sample exhibits a pronounced nonlinear sorption isotherm. The nonlinearity results from the occurrence of two different adsorption modes. The specific host−guest interactions dominate at low concentrations

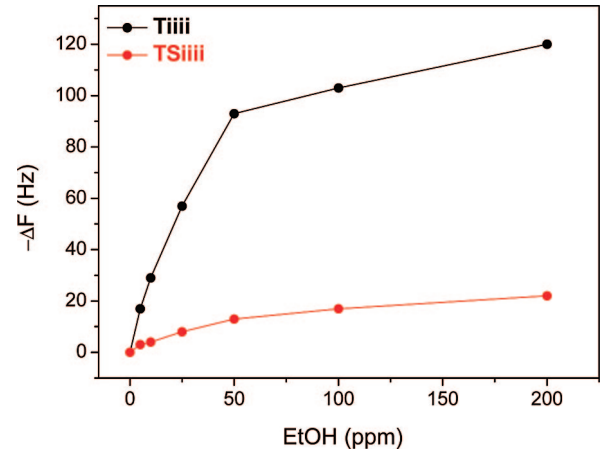

Figure 6. Effect of the EtOH concentration on the resonance frequency of **Tiiii** and **TSiiii** vacuum-evaporated films.

(Langmuir-type behavior), whereas at high concentrations, saturation of the specific sites takes place and nonspecific interactions dominate. Under these conditions the slope ($\Delta f = f(c)$) becomes constant (Henry-type behavior).

The overall shape of the curve can be described by assuming a combined Langmuir- and Henry-type interaction. This concept was previously applied to illustrate the inclusion of inhalation anesthetics onto cyclodextrins.[30] In this model the overall sensor signal Δf is expressed as

$$\Delta f_{\text{sum}} = \Delta f_{\text{Langmuir}} + \Delta f_{\text{Henry}} = K_1 \frac{K' c}{1 + K' c} + K_2 c \qquad (4)$$

where c denotes the analyte concentration, K_1 and K_2 are constants, and K' is the ratio of the kinetic constants of the adsorption and desorption process of alcohol molecules interacting with the recognition site. On the other hand, **TSiiii** layer shows a Henry-type behavior across the entire concentration range, indicating that its sorption process is dominated by unspecific interactions.

These findings, in agreement with the Elovichian data, indicate that although **TSiiii** films are characterized mainly by nonspecific extracavity adsorption, **Tiiii** layers feature intracavity complexation of EtOH.

Enrichment factors (volume concentration in the layer divided by volume concentration in the gas) for **Tiiii** and **TSiiii** exposed to low EtOH concentrations were also calculated using the initial slope. This can be expressed by the curve parameters as

$$\left(\frac{\mathrm{d}\Delta f_{\text{sum}}}{\mathrm{d}c}\right)_{c=0} = K_1 K' + K_2 \qquad (5)$$

Considering a signal-to-noise ratio of three and a noise level of 0.5 Hz, the EtOH limits of detection were calculated to be 0.4 ppm for **Tiiii** and 2.5 ppm for **TSiiii**.

The superior sensing performances of VE coated **Tiiii[H, CH_3, Ph]** sensor have been demonstrated by comparing its responses to those of the spin-coated long chain analogue **Tiiii[$C_{11}H_{23}$, H, Ph]**, the best performer to date.[11] The traces reported in Figure 7 show that the combination of **Tiiii[H, CH_3, Ph]** receptor with VE deposition doubles the EtOH

(29) Toth, J. *Acta Chim., Acad. Sci. Hung.* **1971**, *69*, 311.

(30) Bodenhöfer, K.; Hierlemann, A.; Juza, M.; Schurig, V.; Göpel, W. *Anal. Chem.* **1997**, *69*, 4017.

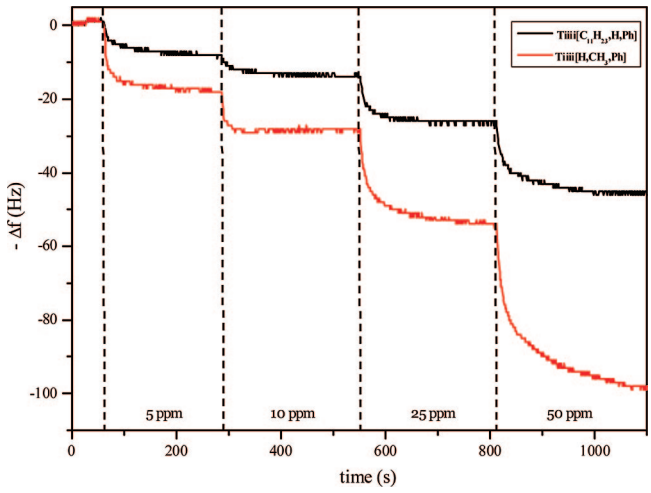

Figure 7. QCM traces of **Tiiii[$C_{11}H_{23}$, H, Ph]** and **Tiiii[H, CH_3, Ph]** sensor responses at increasing amount of EtOH.

sensor sensitivity in the 5−50 ppm range. Above 50 ppm, nonspecific extracavity adsorption becomes significant (Figure 6). This result is remarkable, as it was obtained without altering the receptor site responsible for the alcohol complexation at the gas−solid interface. The application of VE deposition to phosphonate cavitands has provided a significant improvement of their performances as sensitive layers in mass sensors, reducing at the same time the incidence of aspecific adsorption.

4. Conclusions

Tiiii[H, CH_3, Ph] cavitand represents the ultimate receptor for supramolecular mass sensing of short chain alcohols. The excision of the alkyl chains at the lower rim reduces the nonspecific interactions in the layer to a minimum, concomitantly increasing the number of cavities present for the same deposited mass. The unavoidable drawback of this optimization procedure is the very low solubility of cavitands in organic solvents, precluding their deposition on QCM transducers via either spray or spin coating. This problem has been overcome by the use of VE evaporation technique, providing high uniformity and homogeneity of the deposited layers as additional bonuses. The layer roughness, determined by the deposition rate, can be easily controlled by changing the crucible temperature.

Langmuir−Henry isotherms and Elovich kinetics were used to elucidate the different sorption processes occurring onto the different layers. The **TSiiii** layers operate exclusively via nonspecific extracavity adsorption, while in the **Tiiii** films, extracavity adsorption coexists with intracavity complexation. The latter dominates at low analyte concentrations (up to 50 ppm). Kinetically, the release of the complexed EtOH is slower than the interstitial desorption, consistent with the different energy profiles of the two interactions. It must also be emphasized that the mode of complexation is fast and reversible at room temperature, making the resulting sensor fully reliable.

This integrated approach, where both the molecular and the materials properties of the sensing layers have been finely tuned, produced supramolecular mass sensors with improved performances over the existing ones (see Figure 7). This approach can be easily extended to many different classes of organic receptors, opening the way for the rational design of sensor materials in relation to the analytes to be detected.

Acknowledgment. This research was financially supported by the Fifth Commission of Istituto Nazionale di Fisica Nucleare (DEGIMON project) and by the European network of Excellence MAGMANet (M.M. and E.D.). One of the authors thanks Prof. Sarina for her shining mind and irreplaceable role.

Supporting Information Available: Indexed FT-IR bands and ESI-MS spectra of **Tiiii** and **TSiiii** synthesized powders and vacuum-evaporated samples (PDF). This material is available free of charge via the Internet at http://pubs.acs.org.

CM801778F